The temperature dependent optical and scintillation characterisation of Bridgman grown $CsPbX_3$ (X = Br, Cl) single crystals

van Blaaderen, J. Jasper; Biner, Daniel; Krämer, Karl W.; Dorenbos, Pieter

DOI
10.1016/j.nima.2024.169322

Publication date
2024

Document Version
Final published version

Published in
Nuclear Instruments and Methods in Physics Research, Section A: Accelerators, Spectrometers, Detectors and Associated Equipment

Citation (APA)
van Blaaderen, J. J., Biner, D., Krämer, K. W., & Dorenbos, P. (2024). The temperature dependent optical and scintillation characterisation of Bridgman grown $CsPbX_3$ (X = Br, Cl) single crystals. *Nuclear Instruments and Methods in Physics Research, Section A: Accelerators, Spectrometers, Detectors and Associated Equipment*, *1064*, Article 169322. https://doi.org/10.1016/j.nima.2024.169322

Nuclear Instruments and Methods in Physics Research A 1064 (2024) 169322

Contents lists available at ScienceDirect

Nuclear Inst. and Methods in Physics Research, A

journal homepage: www.elsevier.com/locate/nima

Full Length Article

The temperature dependent optical and scintillation characterisation of Bridgman grown $CsPbX_3$ (X = Br, Cl) single crystals

J. Jasper van Blaaderen [a,*], Daniel Biner [b], Karl W. Krämer [b], Pieter Dorenbos [a]

[a] Delft University of Technology, Faculty of Applied Sciences, Department of Radiation Science and Technology, Mekelweg 15, 2629 JB Delft, Netherlands
[b] University of Bern, Department of Chemistry and Biochemistry, Freiestrasse 3, Bern, Switzerland

ARTICLE INFO

Keywords:
Scintillation
3D perovskite
Scintillator
Single crystal
Luminescence
Perovskite

ABSTRACT

Lead halide perovskites are reportedly a very promising group of materials for scintillation due to their fast sub-nanosecond exciton luminescence, small band-gaps, and high theoretical light yield. Unfortunately, they only show emission at cryogenic temperatures. In this work single crystals of $CsPbBr_3$ and $CsPbCl_3$ are studied at cryogenic temperatures. Upon comparing the 10 K emission spectra measured under X-ray and UV–vis excitation, a new near-infrared emission was found for both $CsPbBr_3$ and $CsPbCl_3$ only present under X-ray excitation. The integral light yields of $CsPbBr_3$ and $CsPbCl_3$ at 10 K are estimated to be 34,000 and 2,200 photons/MeV under 40 keV X-ray excitation, respectively. The main components of the light yield of $CsPbBr_3$ at 10 K are the near band-gap free exciton emission that suffers from self-absorption and the broad near-infrared emission that falls outside the typical detection range of a photo-multiplier tube. Due to the combination of the two aforementioned effects it was not possible to measure a γ-ray pulse height spectrum for $CsPbBr_3$ at 10 K. Despite all the suitable properties, like the fast decay, a small band-gap, and the positive prospects of 3D perovskite based scintillators, we conclude that these materials perform poorly as scintillation crystals.

1. Introduction

Lead based halide perovskites are studied and used in many different optoelectronic applications [1–3]. Due to their fast excitonic emission, perovskites [4,5] and perovskite related compounds [6–10] gained interest in the field of scintillation. A clear distinction should be made between true perovskites and perovskite related compounds, as elaborately discussed by Akkerman and Manna [11]. The small band-gap of these materials, around 3 eV, significantly increases their theoretical maximum light yield compared to traditional scintillators [4,12,13]. Based on Eq. (1), the maximum possible light yield is estimated around 130,000 photons/MeV.

$$N_{eh} = \frac{1,000,000}{\beta E_g} \quad (e-h\ pairs/\mathrm{MeV}) \tag{1}$$

Here N_{eh} represents the number of electron–hole pairs created in the scintillator, β is taken to be ≈ 2.5, and E_g represents the band-gap. Lead halide perovskites differ from traditional impurity activated scintillators [12,14–17], by being intrinsic scintillators. Perovskites are defined by an ABX_3 stoichiometry, consisting of a three dimensional corner sharing network of BX_6 octahedra. Often they have been studied in the form of thin films and nanocrystals [18–20].

Lead halide perovskites, both organic–inorganic and completely inorganic compounds, have also been explored for their use in direct radiation detection [21–26]. In this application, the energy deposited by X-rays and γ-photons is converted into a charge pulse. For indirect detection, or scintillation, the energy deposited by X-rays and γ-photons is first converted into a pulse of light. This requires the use of single crystalline materials.

Unfortunately, perovskites show no room temperature emission, which is ascribed to thermal quenching of the exciton luminescence and a small Stokes shift [27–29]. Williams et al. [27] and Wolszscak et al. [28] have proposed several strategies to overcome these problems at room temperature. Examples are using nano materials, doping bulk crystals with activator ions, or utilising the formation of self trapped excitons in lower dimensional compounds. The difference between lower dimensional and nano-structured perovskites is discussed elaborately by Zhou et al. [30].

Another approach to utilise the small band-gap and fast exciton luminescence of perovskites for scintillation is to operate the detector system at cryogenic temperatures. This approach has been explored by Mykhaylyk et al. using $CsPbBr_3$ and $CsPbCl_3$ [5,31]. These inorganic compounds have a higher X-ray absorption and better chemical stability compared to their organic–inorganic counterparts used for

* Corresponding author.
E-mail address: j.j.vanblaaderen@tudelft.nl (J.J. van Blaaderen).

https://doi.org/10.1016/j.nima.2024.169322
Received 18 March 2024; Received in revised form 2 April 2024; Accepted 4 April 2024
Available online 30 April 2024

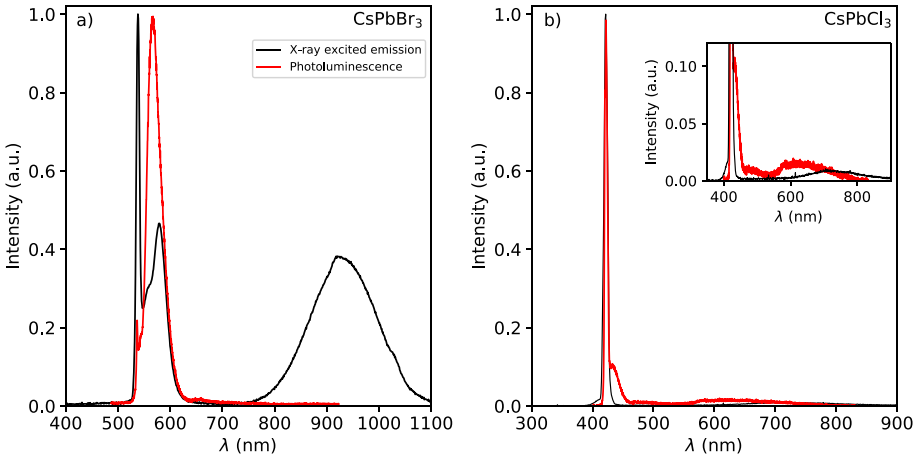

Fig. 1. (a) X-ray excited emission (black line) and photoluminescence emission (red line, λ_{ex} = 310 nm (4 eV)) of $CsPbBr_3$ at 10 K. (b) X-ray excited emission (black line) and photoluminescence emission (red line, λ_{ex} = 354 nm (3.5 eV)) of $CsPbCl_3$ at 10 K. The inset shows a zoom in of both spectra.

direct detection. Mykhaylyk et al. performed low temperature X-ray excited emission and decay measurements, focusing on the fast excitonic emission [5,31].

In this work, single crystals of the inorganic perovskites $CsPbBr_3$ (4.57 g/cm^3) and $CsPbCl_3$ (4.21 g/cm^3) are characterised as function of temperature using a combination of X-ray excitation and UV–vis excitation techniques. Both exhibit an orthorhombic $GdFeO_3$-type perovskite structure with corner-sharing $PbX_{6/2}$ octahedra at room temperature and down to 4 K [32,33]. In contrast, $CsPbI_3$ adopts an orthorhombic $(NH_4)CdCl_3$-type structure with edge-sharing octahedra at room temperature [34]. Hence only the bromide and chloride based caesium lead perovskites are studied. The goal of this work is to develop a better understanding of the low temperature scintillation and optical properties of $CsPbBr_3$ and $CsPbCl_3$ single crystals grown from the melt.

2. Results

Fig. 1a shows the photoluminescence and X-ray excited emission spectra of $CsPbBr_3$ measured at 10 K. The photoluminescence spectrum contains three bands at 535, 544, and 568 nm. These bands were also observed by Nitsch et al. and Dendebera et al. for melt grown $CsPbBr_3$ single crystals [35,36]. The 535 nm peak can be assigned to free exciton emission [36–40]. The origin of the 544 nm shoulder peak and 568 nm peak is still under debate. Explanations range from bound exciton emission, indirect radiative transitions from a Rashba minimum, and donor–acceptor emission to self trapped exciton emission [35,41–45].

The 10 K X-ray excited emission spectrum of $CsPbBr_3$ contains four peaks at 538, 555, 580, and 925 nm. The 538 nm peak is assigned to free exciton emission [5,37–40]. The origin of the 555 and 580 nm emissions, similar to the 544 and 568 nm emissions in the photoluminescence spectrum, is still under debate [35,43–45]. The presence and intensity of these emission peaks strongly depend on the used synthesis method, like whether it is grown from solution or from the melt [46,47]. The broad band 925 nm emission is only observed under X-ray excitation and has never been reported before.

Fig. 1b shows the photoluminescence and X-ray excited emission spectra of $CsPbCl_3$ measured at 10 K. The photoluminescence spectrum contains a sharp peak at 420 nm and a broad band around 625 nm. Peters et al., Sebastian et al., and Nikl et al. have suggested that the 420 nm peak is related to bound exciton emission [40,48,49]. On the long wavelength side of the 420 nm peak, a shoulder centred around 435 nm is observed. It is ascribed to trapped exciton emission [31,48]. The 625 nm emission peak is ascribed to defect related emission [50,51]. Kobayashi et al. observed that the yellow colour of the crystals correlates with the intensity of the 625 nm band [50].

The 10 K X-ray excited emission spectrum of $CsPbCl_3$ contains a single sharp peak at 422 nm and a broad band at 710 nm. Similarly to the 420 nm emission observed in the photoluminescence spectrum, the 422 nm emission is attributed to bound exciton emission [40,48]. The shift of the 625 nm emission observed under UV–vis excitation to 710 nm under X-ray excitation has not been observed before.

To further study the new near infrared emissions observed under X-ray excitation, a series of photoluminescence emission spectra were recorded using excitation energies ranging from 3 eV to 10 eV at 10 K. The respective spectra for $CsPbBr_3$ and $CsPbCl_3$ are shown in Fig. 2a and 2b. The reported band-gaps of $CsPbBr_3$ and $CsPbCl_3$ are 2.4 eV and 3 eV, respectively [52–54]. Hence the lowest excitation energy excites electrons just above the conduction band edge, while the highest excitation energy excites electrons far into the conduction band. The broad near infrared emission bands observed under X-ray excitation are absent within this excitation energy range.

The temperature dependent X-ray excited emission spectra and the respective quenching curves of the integrated peak intensities of $CsPbBr_3$ are shown in Fig. 3a and 3b. The 538, 555, and 580 nm emissions undergo strong thermal quenching below 100 K. The intensity of the 925 nm emission increases upon heating from 10 K, reaching its maximum at 60 K. Above 60 K the emission starts to quench. Based on the quenching curves, shown in Fig. 3b, the temperatures (T_{50}) at which the intensity drops below 50% of the maximum intensity are determined. T_{50} values of 35, 25, 25, and 135 K were determined for the 538, 555, 580, and 925 nm emissions, respectively. The relative contributions of the different emissions to the total intensity at 10 K under X-ray excitation are determined to be 1, 0.7, 1.7, and 7.6 for the 538, 555, 580, and 925 nm emissions, respectively.

The temperature dependent X-ray excited emission spectra and quenching curves of the integrated peak intensities of $CsPbCl_3$ are shown in Fig. 3c and 3d. The 422 nm emission shows strong thermal quenching below 100 K. The intensity of the 710 nm emission shows similar behaviour as the 925 nm emission observed in $CsPbBr_3$. Its intensity increases upon heating from 10 K, reaching its maximum at 75 K. Above this temperature the emission starts to quench. Based on the quenching curves, shown in Fig. 3d, T_{50} values of 45 and 105 K were determined for the 422 and 710 nm emissions, respectively. The relative contributions of the 422 and 710 nm emissions to the total intensity at 10 K under X-ray excitation were determined to be 1 and 0.28, respectively.

The temperature dependent pulsed X-ray excited decay curves of the 538 nm emission of $CsPbBr_3$ are shown in Fig. 4a. Upon heating from 10 to 75 K, the decay time decreases from 440 to 330 ps. This matches with the measurements presented by Mykhaylyk et al. [5]. The decay curves shown in Fig. 4b where recorded by placing a 550 nm

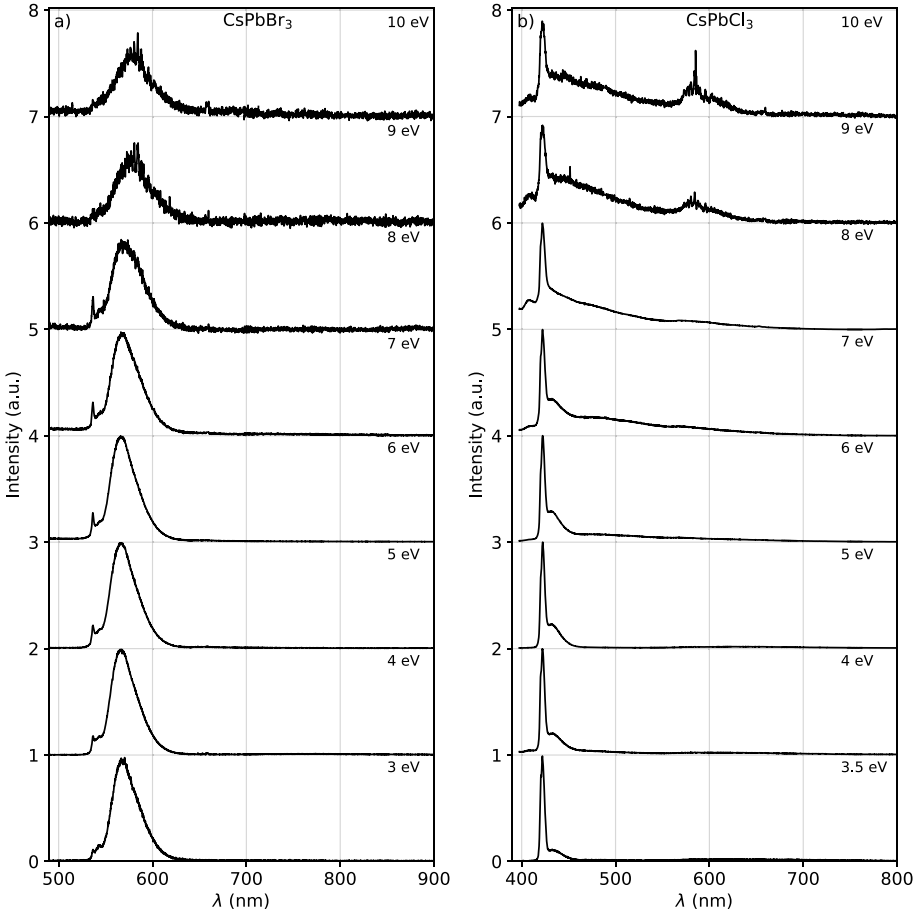

Fig. 2. (a) Photoluminescence emission spectra of $CsPbBr_3$ at 10 K recorded using excitation energies from 3 eV to 10 eV. (b) Photoluminescence emission spectra of $CsPbCl_3$ at 10 K recorded using excitation energies from 3.5 eV to 10 eV.

long pass filter in front of the detector. Now the decay curve shows two components. The fast component is an artefact from part of the 538 nm emission leaking through the long pass filter. The slow component, with a life time of 36 ns, results from both the 555 and 580 nm emissions. The life time of these emissions decreases to 22.5 ns at 25 K.

The temperature dependent pulsed X-ray excited decay curves of the 422 nm emission of $CsPbCl_3$ are shown in Fig. 4c. From 10 to 25 K the decay time increases slightly from 440 ps to 460 ps. Upon heating from 25 to 75 K the decay time decreases to 260 ps. A similar trend is observed in the quenching curves shown in Fig. 3d. This behaviour matches the measurements presented by Mykhaylyk et al. [31].

3. Discussion

Upon exciting $CsPbBr_3$ and $CsPbCl_3$ with X-rays, as shown in Fig. 1a and 1b, near infrared emissions are observed at 925 nm and 710 nm, respectively. These emissions are not present under UV–vis excitation, even upon using excitation energies of 3 to 4 times the band-gap energy. Upon excitation with an X-ray photon all X-ray energy is transferred to an electron. This so called primary electron subsequently excites secondary electrons, via electron–electron interactions. This creates spatially separated electrons and holes, originating from states deep in the conduction and valence band, that need to meet each other to form electron–hole pairs. The free electrons, created under X-ray excitation, have a larger mobility compared to holes and diffuse further away from the initial ionisation track [55–58]. Moreover, X-rays create excitations in the bulk of the crystal. Upon excitation with UV–vis photons however, electron–hole pairs, or excitons, are formed directly. The resulting exciton formation happens on a shorter time scale compared to the recombination of spatially separated electrons and holes. The excitons, upon excitation with UV–vis photons, are created close to the surface of the crystal.

Based on the different excitation mechanisms described above two potential explanations can be formulated for the origin of the near infrared emissions based on the transport of the spatially separated electrons and holes. The free holes have sufficient lifetime to be trapped on a F centre or to self-trap. F centres are colour centres were an electron is trapped on a halide vacancy. After capturing a hole a F^+ centre is created. Sequentially the F^+ centre can trap a conduction band electron to form an excited F centre that emits a photon.

The other potential origin of the near-infrared emissions is self-trapping. This is an intrinsic effect where a free hole first forms a V_k centre. A conduction band electron can then recombine with the V_k centre to form a self-trapped exciton (STE) [59]. The 710 nm and 925 nm emissions observed under X-ray excitation of $CsPbCl_3$ and $CsPbBr_3$ have a full width at half maximum of 0.42 eV and 0.21 eV, respectively. Based on the respective band-gaps, 2.4 eV and 3 eV, the Stokes shifts are determined to be 1.25 eV and 1.06 eV [52–54]. These are typical values for both F-centre emission and STE emission [60,61].

We estimated the scintillation light yields of $CsPbBr_3$ and $CsPbCl_3$ at 10 K by comparing the intensity of their X-ray excited emission spectra, measured using an average X-ray energy of 40 keV, to that of $CsCu_2I_3$ [10]. The estimated integral scintillation light yields were determined to be 34,000 and 2,200 photons/MeV for $CsPbBr_3$ and $CsPbCl_3$, respectively. These numbers are much lower than the theoretical maximum of 166,000 and 133,000 photons/MeV estimated based on the band-gaps of $CsPbBr_3$ and $CsPbCl_3$ with Eq. (1), respectively. The contributions from the different emission to the total estimated

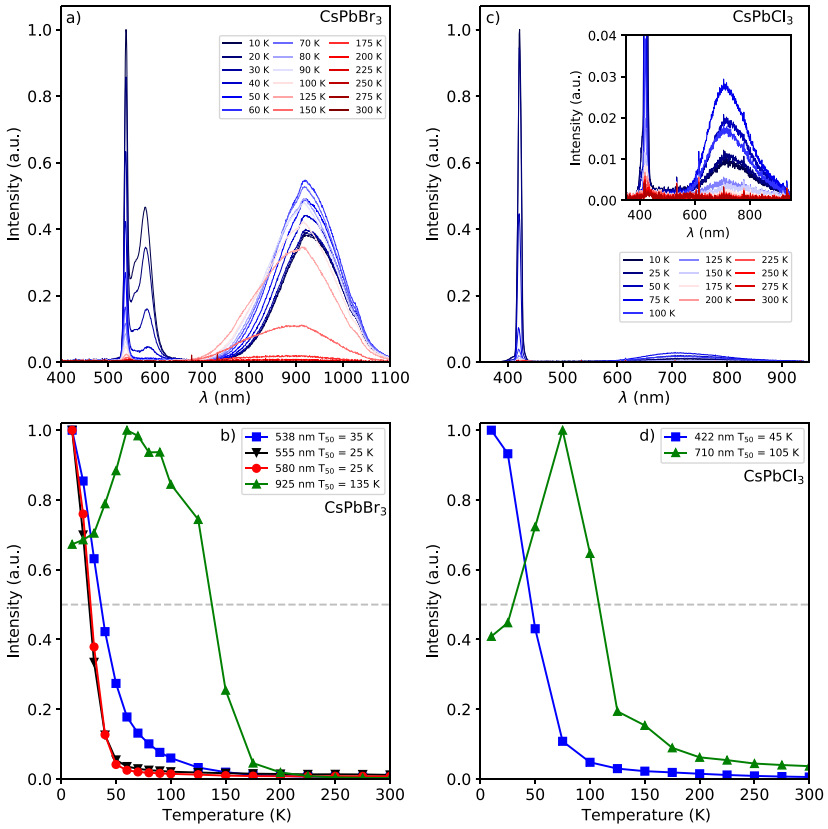

Fig. 3. (a) Temperature dependent X-ray excited emission spectra of $CsPbBr_3$ measured from 10 K to 300 K. (b) Temperature dependent integrated emission intensities of the 538 nm, 555 nm 580 nm, and 925 nm emissions of $CsPbBr_3$ (c) Temperature dependent X-ray excited emission spectra of $CsPbCl_3$ measured from 10 K to 300 K. (d) Temperature dependent integrated emission intensities of the 422 nm and 710 nm emissions of $CsPbCl_3$.

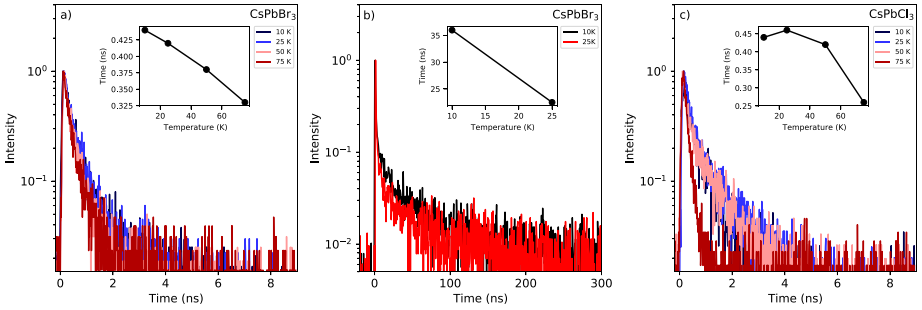

Fig. 4. (a) Temperature dependent pulsed X-ray excited decay spectra of the 538 nm emission of $CsPbBr_3$ between 10 K and 75 K. The inset shows the temperature dependent change of the life time. (b) Temperature dependent pulsed X-ray excited decay spectra of $CsPbBr_3$ in which the 538 nm emission is filtered out by placing a 550 nm long pass filter in front of the detector. The inset shows the temperature dependent change of the life time. (c) Temperature dependent pulsed X-ray excited decay spectra of the 422 nm emission of $CsPbCl_3$ between 10 K and 75 K. The inset shows the temperature dependent change of the life time.

light yields are calculated based on the relative intensities in Fig. 1, as summarised in Table 1. The estimated light yield of $CsPbCl_3$ at 10 K is approximately 1.3% of its calculated maximum theoretical value. The main contribution is from its 422 nm emission. For $CsPbBr_3$ the estimated light yield at 10 K is approximately 25.5% of its calculated maximum theoretical value. The main contribution is from its 925 nm emission. Both compounds have also been used to measure 662 keV γ-photon excited pulse height spectra at 10 K; a 662 keV photopeak could not be distinguished from the background.

The estimated light yields summarised in Table 1 were determined based on the X-ray excited emission spectra using an average X-ray energy of 40 keV. The calculated attenuation length for 40 keV photons in $CsPbCl_3$ and $CsPbBr_3$ are approximately 250 μm. The 662 keV γ-photon used in the pulse height measurement on the other hand excite the bulk of the crystal.

Mykhaylyk et al. reported light yields of 109.000 and 47.000 photons/MeV for $CsPbBr_3$ and $CsPbCl_3$ at 7 K, respectively [5,31]. These numbers were estimated by comparing a pulse height spectrum, recorded under alpha excitation of ^{241}Am at 7 K, of $CsPbBr_3$ and $CsPbCl_3$ to that of LYSO. The later has a light yield of 34.000 photons/MeV under γ-ray excitation. However, under α excitation LYSO is much less efficient. With an α/β ratio of 0.14 from Wolszczak et al. [62], an α-particle light yield of 4,760 photons/MeV occurs. This aspect was not taken into account by Mykhaylyk et al. [5,31]. The α/β ratio and proportionality of $CsPbBr_3$ and $CsPbCl_3$ is also not known. Mykhaylyk et al., in their publication on $CsPbBr_3$, also estimated the light yield in a similar way as presented in this work, reporting 50.000 photons/MeV [5].

The 10 K X-ray excited emission spectra of both compounds, combined with the typical photo-detection efficiency curve of a photomultiplier tube (PMT), are shown in Fig. 5. The detection efficiency

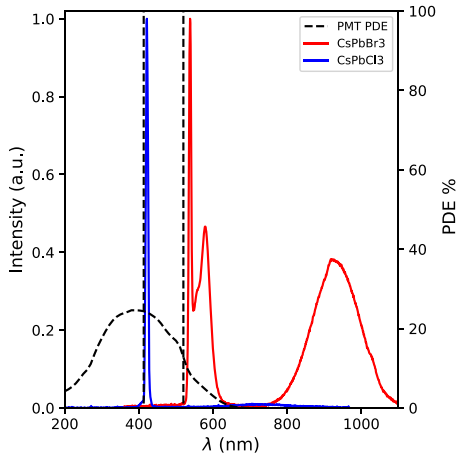

Fig. 5. X-ray excited emission spectra of $CsPbCl_3$ (blue) and $CsPbBr_3$ (red) measured at 10 K compared to the detection efficiency of a Hamamatsu Super Bialkali R6231-100 (SN ZE4500) (black dashed line). The vertical black dashed lines at 413 nm (3 eV) and 520 nm (2.4 eV) represent the band-gaps of $CsPbCl_3$ and $CsPbBr_3$, respectively.

of the PMT drops below 2% at wavelengths longer than 620 nm. This means that the 925 nm emission of $CsPbBr_3$ falls completely outside the detection range, drastically decreasing the number of photons available for detection. The 710 nm emission of $CsPbCl_3$ only partially falls within the low side of detection efficiency. The other emissions, for both compounds, fall withing the detection range of the PMT. However, as discussed by Williams et al. [27] and Wolszscak et al. [28], the exciton emissions close to the band-gap suffer from self-absorption. The band-gaps of both materials with respect to their emissions are represented in Fig. 5 by the vertical dashed lines. Only the 555 and 580 nm emissions from $CsPbBr_3$ have a potentially useful contribution to the light yield. However, as shown in Fig. 5, they emit in the spectral region where the PDE drops below 10%. In total these emissions contribute approximately 7.000 photons/MeV, corresponding with less than 350 detected photons/MeV. This number is further reduced by the presence of tail states, as shown in the room temperature absorbance spectra in Figure S1, and large penetration depth of 662 keV γ-photons increasing the chance of re-absorption. Due to the geometric restrictions needed to perform the measurement at 10 K, the sample could not be mounted directly on the entrance window of the PMT, reducing the light collection efficiency. The absence of a pulse height spectrum at 10 K is thus ascribed to a combination of self-absorption related problems, emission falling outside the PMT detection range, and sub-optimal experimental conditions.

It has been suggested by Stoumpos et al. that the defect related emissions on the long wavelength side of the free exciton emission could be suppressed by growing these materials from solution instead of the melt [46,47]. However, this will not solve any self-absorption related problems of the free exciton emissions [63]. The near infrared emissions, if originating from F-centres might also be suppressed when crystals are produced from solution. Self-trapping however, is an intrinsic effect and will thus not be influenced. Similar problems should be expected for the organic–inorganic methylammonium based perovskites, $CH_3NH_3PbX_3$ (X = Cl, Br, I) which show similar near band-edge emission as the completely inorganic perovskites. Scintillation characterisations have been performed on $CH_3NH_3PbBr_3$ [64,65]. Li et al. demonstrated that $CH_3NH_3PbBr_3$ also shows self-absorption related problems, thus preforming poorly as a scintillator crystal [65].

4. Conclusion

In this work, the inorganic perovskites $CsPbBr_3$ and $CsPbCl_3$ have been studied under X-ray and UV–vis excitation at cryogenic temperatures. Upon comparing the emission spectra measured at 10 K using the different excitation methods, new broad near-infrared emissions were discovered in both compounds. Based on the peak width, large Stokes shift, and red shift of the emission when going from $CsPbCl_3$ to $CsPbBr_3$ it is suggested that it originates from F-centres or self trapping. Both compounds show fast exciton related emissions of approximately 450 ps at 10 K. For $CsPbBr_3$ an additional 36 ns component was measured related to the 555 nm and 580 nm emissions. The light yields of $CsPbBr_3$ and $CsPbCl_3$ were estimated to be 34,000 and 2,200 photons/MeV. In $CsPbBr_3$, the major part of the light yield is emitted in the 925 nm emission band, which falls outside the detection range of a typical photo-multiplier tube. The other emissions suffer from self-absorption. Hence no pulse height spectrum was observed under 662 keV γ-photon excitation at 10 K.

5. Experimental

$CsPbCl_3$ and $CsPbBr_3$ crystals were grown from stoichiometric amounts of the binary halides in sealed silica ampoules by the vertical Bridgman technique. CsCl (Alfa, 5N) and CsBr (Fluka, >99.5%) were dried in high vacuum at 200 °C. $PbCl_2$ and $PbBr_2$ (both Alpha, 5N) were sublimed in a silica apparatus under high vacuum for purification at 480 °C and 375 °C, respectively. Typical batch size was 5 g. The powder was molten up at 30 K above the congruent melting point of $CsPbCl_3$ at 615 °C and $CsPbBr_3$ at 570 ° C, respectively. The temperature was kept for one day and then the crystal growth was started. The furnace was moved upwards by ca. 15 mm/day; samples reached room temperature in about 10 days. Transparent crystal pieces were cleaved from the boule and sealed in silica ampoules under He gas for the

spectroscopic characterisations. All handling of starting materials and products were done under dry conditions in glove boxes or sealed sample containers. Powder X-ray diffraction patterns were measured with Cu $K_{\alpha 1}$ radiation in reflection geometry at room temperature, see Figure S2 and S3 of supporting information. $CsPbCl_3$ and $CsPbBr_3$ adopt the $GdFeO_3$-type perovskite structure at room temperature [32].

The X-ray excited emission spectra were measured using a tungsten anode X-ray tube at an operation voltage of 79 kV. The average X-ray energy from this tube is 40 keV. The low energy X-rays from the spectrum produced by the tube are removed by placing a 3 mm aluminium filter in front of the tube in order to prevent radiation damage to the sample. The crystals were mounted on the cold finger of a closed cycle helium cryostat operating below 10^{-4} bar. The crystal is excited and the emitted light is detected from the same surface; the measurement is performed in reflectivity mode.

The estimated light yields were calculated by comparing the total spectral intensity of the 10 K X-ray excited emission spectra of $CsPbBr_3$ and $CsPbCl_3$ to that of a $CsCu_2I_3$ crystal. The experimental conditions, sample alignment, X-ray fluence, and size of the samples were similar for all three measurements. The scintillation yield of $CsCu_2I_3$ has been determined in a separate experiment under 662 keV γ-photon excitation on an APD as described in Ref. [10]. In Ref. [10] the non-proportionality of $CsCu_2I_3$ was also measured, showing only a 4% difference upon comparing the light yield determined at 60 keV and 662 keV. The spectral intensity is corrected for the detection efficiency.

The photoluminescence emission spectra were measured by exciting the samples either with the light of a 450 W xenon lamp passing through a Horiba Gemini 180 monochromator or by exciting with a Hamamatsu L1835 deuterium lamp passing through an Action Research Corporation VM 502 monochromator. The emission light passed through a Princeton Instruments SpectraPro-SP2358 monochromator and was detected using a Hamamatsu C9100-13 EM CCD. The crystals were mounted on the cold finger of a closed cycle helium cryostat operating below 10^{-4} bar.

The pulsed X-ray decay cures were measured by the time-correlated single photon counting method. A PicoQuant LDH-P-C440M pulsed laser, generating the start signal, directly excites a Hamamatsu N5084 light excited X-ray tube, creating a pulse of X-rays with an average

Table 1
Summary and comparison of the relative intensity of the emissions observed under X-ray excitation and their respective contributions to the total light yield at 10 K, and the attenuation length at 40 keV and 400 keV for $CsPbBr_3$ and $CsPbCl_3$.

		Relative intensity	Light yield Photons/MeV	
$CsPbBr_3$	538 nm	1	3,100	Self-Absorption
	555 nm	0.7	2,200	Useful yield
	580 nm	1.7	5,200	Useful yield
	925 nm	7.6	23,500	Outside PDE PMT
	All		34,000	
	Theoretical		166,000	
$CsPbCl_3$	422 nm	1	1,700	Self-Absorption
	710 nm	0.28	500	Outside PDE PMT
	All		2,200	
	Theoretical		133,000	

energy of 18.2 keV and temporal resolution of 200 ps. The scintillation photons are detected by an ID Quantique id100-50 single-photon counter, which is used as the stop signal. An Ortec 567 time-to-amplitude converter was used to process the start and stop signals. An Ortec AD 144 16 K ADC was used to digitise the signal. The crystals were mounted on the cold finger of a closed cycle helium cryostat operating below 10^{-4} bar. The crystal is excited and the emitted light is detected from the same surface; the measurement is performed in reflectivity mode.

In order to record pulse height spectra at 10 K the samples were mounted on a parabolic stainless steel reflector covered with aluminium foil to improve the light collection efficiency. The reflector was mounted on the cold finger of a closed cycle helium cryostat operating below 10^{-4} bar. A Hamamatsu Super Bialkali R6231-100 (SN ZE4500) PMT was used to detect the scintillation photons. It was placed close to the window on the outside of the sample chamber. The distance between the sample and PMT was approximately 5 cm.

CRediT authorship contribution statement

J. Jasper van Blaaderen: Writing – review & editing, Writing – original draft, Visualization, Validation, Supervision, Project administration, Methodology, Investigation, Formal analysis, Data curation, Conceptualization. **Daniel Biner:** Investigation, Formal analysis. **Karl W. Krämer:** Writing – review & editing, Investigation, Data curation. **Pieter Dorenbos:** Writing – review & editing, Supervision, Project administration, Formal analysis, Conceptualization.

Declaration of competing interest

The authors declare that they have no known competing financial interests or personal relationships that could have appeared to influence the work reported in this paper.

Data availability

Data will be made available on request.

Acknowledgement

The authors acknowledge financial supports from the TTW/OTP grant no. 18040 of the Dutch Research Council.

Appendix A. Supplementary data

Supplementary material related to this article can be found online at https://doi.org/10.1016/j.nima.2024.169322.

References

[1] M.A. Green, A. Ho-Naillie, H.J. snaith, Nat. Photonics 8 (2014) 506, http://dx.doi.org/10.1038/nphoton.2014.134.
[2] X.Y. Chin, D. Cortecchia, J. Yin, A. Bruno, C. Soci, Nature Commun. 6 (2015) 7383, http://dx.doi.org/10.1038/ncomms8383.
[3] L. Dou, Y.M. Yang, J. You, Z. Hong, W.-H. Chang, G. Li, Y. Yang, Nature Commun. 5 (2014) 5404, http://dx.doi.org/10.1038/ncomms6404.
[4] M.D. Bitowosuto, D. Cortecchia, W. Drozdowski, K. Brylew, W. Lachmanski, A. Bruno, C. Soci, Sci. Rep. 6 (2016) 37254, http://dx.doi.org/10.1038/srep37254.
[5] V.B. Mykhaylyk, H. Kraus, V. Kapustianyk, H.J. Kim, P. Mercere, M. Rudko, P. Da Silva, O. Antonyak, M. Dendebera, Sci. Rep. 10 (2020) 8601, http://dx.doi.org/10.1038/s41598-020-65672-z.
[6] F. Maddalena, L. Tjahjana, A. Xie, Arramel, S. Zeng, H. Wong, P. Coquet, W. Drozdowski, C. Dujardin, C. Dang, M.D. Birowosuto, Crystals 9 (2019) 88, http://dx.doi.org/10.3390/cryst9020088.
[7] A. Xie, F. Maddalena, M.E. Witkowski, M. Makowski, B. Mahler, W. Drozdowski, S.V. Springham, P. Coquet, C. Dujardin, M.D. Bitoosuto, C. Dang, Chem. Mater. 32 (2020) 19, http://dx.doi.org/10.1021/acs.chemmater.0c02789.
[8] J.J. van Blaaderen, F. Maddalena, C. Dong, M.D. Birowosuto, P. Dorenbos, J. Mater. Chem. C 10 (2022) 11598–11606, http://dx.doi.org/10.1039/D2TC01483A.
[9] J.J. van Blaaderen, S. van der Sar, D. Onggo, Md Abdul K. Sheikh, D.R. Schaart, M.D. Birowosuto, P. Dorenbos, J. Lumin. 263 (2023) 120012, http://dx.doi.org/10.1016/j.jlumin.2023.120012.
[10] J.J. van Blaaderen, L.A. van den Brekel, K.W. Kramer, P. Dorenbos, Chem. Mater. 35 (2023) 9623–9631, http://dx.doi.org/10.1021/acs.chemmater.3c01810.
[11] A. Akkerman, L. Manna, ACS Energy Lett. 5 (2020) 604–610, http://dx.doi.org/10.1021/acsenergylett.0c00039.
[12] P. Dorenbos, Opt. Mater.: X 1 (2019) 100021, http://dx.doi.org/10.1016/j.omx.2019.100021.
[13] P. Dorenbos, Fundamental limitations in the performance of Ce^{3+}-, Pr^{3+}-, and Eu^{2+}- activated scintillators, IEEE Trans. Nucl. Sci. 57 (2010) 3, http://dx.doi.org/10.1109/TNS.2009.2031140.
[14] C. van Aarle, K.W. Krämer, P. Dorenbos, J. Mater. Chem. C 11 (2023) 2336–2344, http://dx.doi.org/10.1039/D2TC05311J.
[15] C. van Aarle, K.W. Krämer, P. Dorenbos, J. Lumin. 251 (2022) 119209, http://dx.doi.org/10.1016/j.jlumin.2022.119209.
[16] C. van Aarle, K.W. Krämer, P. Dorenbos, J. Lumin. 238 (2021) 118257, http://dx.doi.org/10.1016/j.jlumin.2021.118257.
[17] E.V.D. van Loef, P. Dorenbos, C.W.E. van Eijk, Appl. Phys. Lett. 79 (2001) 1573, http://dx.doi.org/10.1063/1.1385342.
[18] Z. Shaki, M.M. Byranvand, N. Taghavinia, M. Kedia, M. Saliba, Energy Environ. Sci. 14 (2021) 5690–5722, http://dx.doi.org/10.1039/D1EE02018H.
[19] W.A. Dunlap-Shohl, Y. Zhou, N.P. Padture, D.B. Mitzi, Chem. Rev. 119 (2019) 3193–3295, http://dx.doi.org/10.1021/acs.chemrev.8b00318.
[20] Q.A. Akkerman, G. Raino, M.V. Kovalenko, L. Manna, Nature Mater. 17 (2018) 394–405, http://dx.doi.org/10.1038/s41563-018-0018-4.
[21] J. Peng, C.Q. Xia, Y. Xu, R. Li, L. Cui, J.K. Clegg, L.M. Harz, M.B. Johnston, Q. Lin, Nat. Commun. 12 (2021) 153, http://dx.doi.org/10.1038/s41467-021-21805-0.
[22] Y. He, Z. Liu, K.M. McCall, W. Lin, D.Y. Chung, B.W. Wessells, M.G. Kanatzidis, Nucl. Instrum. Methods Phys. Res. A 992 (2019) 217–221, http://dx.doi.org/10.1016/j.nima.2019.01.008.
[23] L. Pan, Y. Feng, P. Kandlakunta, J. Huang, L.R. Cao, IEEE Trans. Nucl. Sci. 67 (2020) 443–449, http://dx.doi.org/10.1109/TNS.2020.2964306.
[24] Y. He, L. Matei, H.J. Jung, K.M. McCall, M. Chen, C.C. Staumpos, z. Liu, J.A. Peters, D.Y. LChung, B.W. Wessels, M.R. Wasielewski, V.P. Dravid, A. Burger, M.G. Kanatzidis, Nature Commun. 9 (2018) 1609, http://dx.doi.org/10.1038/s41467-018-04073-3.

[25] S. Yakunin, D.N. Dirin, Y. Shynkarenko, V. Morad, I. Cherniukh, O. Nazarenko, D. Kreil, T. Nauser, M.V. Kovalenko, Nat Photonics 10 (2016) 585–589, http://dx.doi.org/10.1038/nphoton.2016.139.
[26] H. Wei, Y. Fang, P. Mulligan, W. Chuirazzi, H.-H. Fang, C. Wang, B.R. Ecker, Y. Gao, M.A. Loi, L. Cao, J. Huang, Nat. Photonics 10 (2016) 333–339, http://dx.doi.org/10.1038/nphoton.2016.41.
[27] R.T. Williams, W.W. Wolszczak, X. Yan, D.L. Carrol, ACS Nano 14 (2020) 5161–5169, http://dx.doi.org/10.1021/acsnano.0c02529.
[28] W.W. Wolszczak, D.L. Carrroll, R.T. Williams, Advanced X-Ray Detector Technologies, 2022, http://dx.doi.org/10.1007/978-3-030-64279-2_1, Chapter 1.
[29] F. Staub, I. Anusca, D.C. Lupascu, U. Rau, T. Kirchartz, J. Phys.: Mater. 3 (2020) 2, http://dx.doi.org/10.1088/2515-7639/ab6fd0.
[30] C. Zhou, H. Lin, Q. He, L. Xu, M. Worku, M. Chaaban, S. Lee, X. Shi, M.-H. Du, B. Ma, Mater. Sci. Eng. R 137 (2019) 38–65, http://dx.doi.org/10.1016/j.mser.2018.12.001.
[31] V.B. Mykhaylyk, M. Rudko, H. Kraus, V. Kapustianyk, V. Kolomiets, N. Vitoratou, Y. Chornodolskyy, A.S. Voloshinovskii, L. Vasylechko, J. Mater. Chem. C 11 (2023) 656–665, http://dx.doi.org/10.1039/D2TC04631H.
[32] M.R. Linaburg, E.T. McClure, J.D. Majher, P.M. Woodward, ACS Chem. Mater. 23 (2017) 3507–3514, http://dx.doi.org/10.1021/acs.chemmater.6b05372.
[33] C.A. Lopez, G. Abia, M.C. Alvarez-Galvan, B.-K. Hong, M.V. Martinez-Huerta, F. Serrano-Sanchez, F. Carrascoso, A. Castellanos-Gomez, M.T. Fernandez-Diaz, J.A. Alonso, ACS Omega 5 (2020) 5931–5938, http://dx.doi.org/10.1021/acsomega.9b04248.
[34] Z. Yao, W. Zhao, S. Liu, J. Mater. Chem. A 9 (2021) 11124–11144, http://dx.doi.org/10.1039/D1TA01252E.
[35] K. Nitsch, V. Hamplova, M. Nikl, K. Polak, M. Rodava, Chem. Phys. Lett. 258 (1996) 518–522, http://dx.doi.org/10.1016/0009-2614(96)00665-3.
[36] M. Dendebera, Y. Chornodolskyy, R. Gamernyk, O. Antonyak, I. Pashuk, S. Myagkota, I. Gnilitskyi, V. Pankratov, V. Vistovskyy, V. Mykhaylyk, M. Grinberg, J. Lumin. 225 (2020) 117346, http://dx.doi.org/10.1016/j.jlumin.2020.117346.
[37] J.A. Steele, P. Puech, B. Monserrat, B. Wu, R.X. Yang, T. Kirchartz, H. Yuan, G. Fleury, D. Giovanni, E. Fron, M. Keshavarz, E. Debroye, G. Zhou, T.C. Sum, A. Walsh, J. Hofkent, M.B.J. Roeffaers, ACS Energy Lett. 4 (2019) 2205–2212, http://dx.doi.org/10.1021/acsenergylett.9b01427.
[38] W. Du, S. Zhang, Z. Wu, Q. Shang, Y. Mi, J. Chen, C. Qin, X. Qiu, Q. Zhang, X. Liu, Nanoscale 11 (2019) 3145–3153, http://dx.doi.org/10.1039/C8NR09634A.
[39] C. Wolf, T.-W. Lee, Materialstoday Energy 7 (2018) 199–207, http://dx.doi.org/10.1016/j.mtener.2017.09.010.
[40] M. Sebastian, J.A. Peters, C.C. Stoumpos, J. Im, S.S. Kostina, Z. Liu, M.G. Kanatzidis, A.J. Freeman, B.W. Wessels, Phys. Rev. B 92 (2015) 235210, http://dx.doi.org/10.1103/PhysRevB.92.235210.
[41] X. Fang, K. Zhang, Y. Li, L. Yao, Y. Zhang, Y. Wang, W. Zhai, L. Tao, H. Du, G. Ran, Appl. Phys. Lett. 108 (2016) 071109, http://dx.doi.org/10.1063/1.4942410.
[42] E.M. Hutter, M.C. Gelvez-Rueda, A. Osherov, V. Bulovic, F.C. Grozema, S.D. Stranks, T.J. Savenije, Nature Mater. 16 (2017) 115–120, http://dx.doi.org/10.1038/nmat4765.
[43] X. Lao, Z. Yang, Z. Su, Z. Wang, H. Ye, M. Wang, X. Yao. S. Xu, Nanoscale 10 (2018) 9949–9956, http://dx.doi.org/10.1039/C8NR01109E.
[44] H. Linnenbank, M. Saliba, L. Gui, B. Metzger, S.G. Tikhodeev, J. Kadro, G. Nasti, A. Abate, A. Hagfeldt, M. Graetzel, G. Giessen,
[45] T.M. Demkiv, S.V. Myagkota, T. Malyi, A.S. Pushak, V.V. Vistovskyy, P.M. Yakibchuk, O.V. Shapoval, N.E. Mitina, A.S. Zaichenko, A.S. voloshinovskii, J. Lumin. 198 (2018) 103–107, http://dx.doi.org/10.1016/j.jlumin.2018.02.021.
[46] C.C. Stoumpos, M.G. Kanatzidis, Acc. Chem. Res. 48 (2015) 2791–2802, http://dx.doi.org/10.1021/acs.accounts.5b00229.
[47] C.C. Stoumpos, C.D. Malliakas, J.A. Peters, Z. Liu, M. Sebastian, J. Im, T.C. Chasapis, A.C. Wibowo, D.Y. Chung, A.J. Freeman, B.W. Wessels, M.G. Kanatzidis, Crystal Growth Des. 13 (2013) 2722–2727, http://dx.doi.org/10.1021/cg400645t.
[48] J.A. Peters, Z. Liu, M.C. De Siena, M.G. Kanagzidis, B.W. Wessels, J. Lumin. 243 (2022) 118661, http://dx.doi.org/10.1016/j.jlumin.2021.118661.
[49] M. Nikl, E. Mihokoba, K. Nitsch, K. Polak, M. Rodova, M. Dusek, G.P. Pazzi, P. Fabeni, L. Salvini, M. Gurioli, Chem. Phys. Lett. 220 (1994) 1–2, http://dx.doi.org/10.1016/0009-2614(94)00127-8.
[50] M. Kobayashi, K. Omata, S. Sigimoto, Y. Tamagawa, T. Kuroiwa, H. Asada, H. Takeuchi, S. Kondo, Nucl. Instrum. Methods Phys. Res. A 592 (2008) 369–373, http://dx.doi.org/10.1016/j.nima.2008.04.079.
[51] K. Watanabe, M. Koshimizu, T. Yanagida, Y. Fujimoto, K. Asai, Japan. J. Appl. Phys. 55 (2016) 0BC20, http://dx.doi.org/10.7567/JJAP.55.02BC20.
[52] T. Ma, S. Wang, Y. Zhang, K. Zhang, L. Yi, J. Mater. Sci. 55 (2020) 464–479, http://dx.doi.org/10.1007/s10853-019-03974-y.
[53] L.Y. Bai, S.W. Wang, Y.W. Zhang. K. X. Zhang, L.X. and Yi, J. Luminesence 227 (2020) 117592, http://dx.doi.org/10.1016/j.jlumin.2020.117592.
[54] K. Heidrich, H. Kunzel, J. Treusch, Solid State Commun. 25 (1978) 887–889, http://dx.doi.org/10.1016/0038-1098(78)90294-6.
[55] R.T. Williams, J.Q. Grim. Q. Li, K.B. Ucer, W.W. Moses, Basic Solid State Phys. 248 (2011) 426–438, http://dx.doi.org/10.1002/pssb.201000610.
[56] W.W. Moses, G. Bizarri, R.T. Williams, S.A. Payne, A.N. Vasilev, J. Singh, Q. Li, J.Q. Grim, W.-S. Choong, IEEE Trans. Nuclear Sci. 59 (2012) 2038–2044, http://dx.doi.org/10.1109/TNS.2012.2186463.
[57] A.N. Vasilev, IEEE Trans. Nucl. Sci. 55 (2008) 3, http://dx.doi.org/10.1109/TNS.2007.914367.
[58] I.V. Khodyuk, Nonproportionality of Inorganic Scintillators, ISBN: 9789088915536, http://dx.doi.org/10.4233/uuid:cb4008a8-981a-4283-b213-199d41756269.
[59] K.S. Song, R.T. Williams, Self Trapped Excitons, in: Springer Series in Solid-State Sciences, vol. 105, ISBN: 3-540-55906-X, 1993.
[60] F. Agullo-Lopez, C.R.A. Catlow, D.P. townsend, Point Defects in Materials, 1998, Chapter 5, IDBN 0-12-044510-7.
[61] S. Li, J. Luo, J. Liu, J. Tang, J. Phys. Chem. Lett. 10 (2019) 1999–2007, http://dx.doi.org/10.1021/acs.jpclett.8b03604.
[62] W. Wolszczak, P. Dorenbos, IEEE Trans. Nucl. Sci. 64 (2017) 6, http://dx.doi.org/10.1109/TNS.2017.2699327.
[63] S. Gull, M.H. Jamil, X. Zhang, H.-S. Kwok, G. Li, Chem. Open 11 (2022) 3, http://dx.doi.org/10.1002/open.202100285.
[64] V.B. Mykhaylyk, H. Kraus, M. Saliba, Mater. Horiz. 6 (2019) 1740–1747, http://dx.doi.org/10.1039/C9MH00281B.
[65] Y. Li, W. Shao, X. Ouyang, Z. Zhu, H. Zhang, X. Ouyang, B. Liu, Q. Xu, J. Phys. Chem. C 123 (2019) 28, http://dx.doi.org/10.1021/acs.jpcc.9b05269.